

theory (for strong interactions), then these terms are again no more than logarithmically divergent. Thus again Fig. 1 (b) represents the leading contribution to the electromagnetic mass difference and again Eq. (5) may be expected to hold for very large Λ^2 .

For a photon cutoff momentum of the order of 1 Bev/c, deviation from (5) will occur that we cannot estimate, whereas for point interactions (5) is exact up to finite α corrections to m_π/m_K .²

It is a pleasure for one of us (S.G.) to thank Professor Ferretti and CERN for their hospitality

*National Science Foundation Fellow. On leave from the Radiation Laboratory, Berkeley, California.

¹R. Feynman and G. Speisman, Phys. Rev. 94, 500 (1954); A. Petermann, Helv. Phys. Acta 27, 441 (1954).

²One can actually show that terms $\sim (\Lambda^2/m)\log(\Lambda^2/m^2)$ do never occur.

PHOTOPRODUCTION OF SINGLE POSITIVE PIONS FROM HYDROGEN IN THE 600- TO 1000-Mev REGION*

F. P. Dixon and R. L. Walker
California Institute of Technology,
Pasadena, California

(Received November 17, 1958)

The earlier magnetic spectrometer measurements¹ of pions from the reaction $\gamma + p \rightarrow \pi^+ + n$, initiated by the bremsstrahlung beam of the Cal-Tech Synchrotron in a liquid hydrogen target, have been extended to cover a range of 20° to about 163° in the center-of-momentum system for laboratory photon energies of 600, 700, 800, 900, and 1000 Mev. The experimental technique was improved by the placement of veto counters along the pole faces of the magnet to eliminate counts from scattered particles and from showers produced in the iron. Also, a Lucite Čerenkov counter was used to discriminate against protons, which could not be clearly separated from pions at momenta above 800 Mev/c by a pulse-height analysis. New data at angles greater than 135° were taken with the same medium-momentum spectrometer used for the previous measurement. However, for pion momenta greater than 600 Mev/c (forward angles) the high-momentum spectrometer described by Vette² was employed with the addition of the pole face veto counters and a front "aperture" counter located near the magnet entrance.

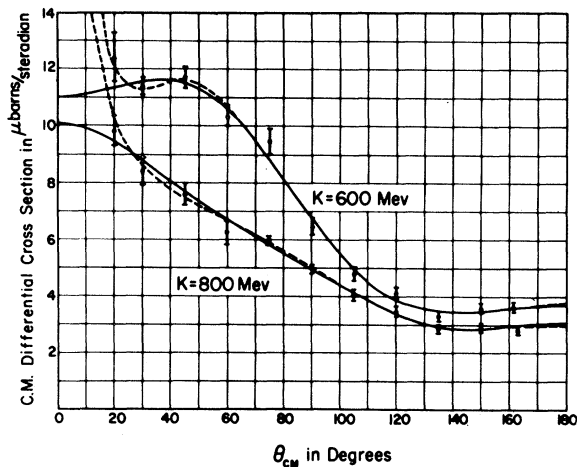


FIG. 1. Angular distributions of pions from $\gamma + p \rightarrow \pi^+ + n$ for 600- and 800-Mev photons. The solid curves in Figs. 1-3 are least-squares fits to the data, of the form $d\sigma/d\Omega = \sum_{n=0}^4 A_n \cos^n \theta$. The dashed curves are fits of the form $(1 - \beta \cos \theta)^2 (d\sigma/d\Omega) = \sum_{n=0}^6 B_n \cos^n \theta$ following Moravcsik.⁴

The data presented in this report have been corrected for empty-target backgrounds, pion decay in flight, absorption of pions in the system, and muon contamination. The background was found to be about 10% of the total counting rate. The worst case was 13% at 11.3° in the laboratory system. Negative-field runs at this position showed no contribution from the hydrogen, since empty- and full-target runs gave equal counting rates amounting to 4% of the total positive-field run with hydrogen in the target. The absorption correction was 14%, where the geometrical value was used for the counters and the attenuation in the half-inch Pb absorber was measured. A preliminary estimate of muon contamination was used and gave 4 ± 2 to $8 \pm 4\%$ correction for this effect. With the pion decay loss this resulted in a net correction of 8 to 19% for effects associated with pion decay.

Angular distributions in the center-of-momentum system for each of the five photon energies investigated are shown in Figs. 1-3. In these figures the previous cross sections of reference 1 have been increased about 4% as a result of a recent beam monitor calibration.³ None of the data should be considered as final, since we plan to make an improved calculation of the corrections for muon contamination, and a future detailed measurement of the bremsstrahlung spectrum could result in some changes in the cross sections. We have used essentially a thin-

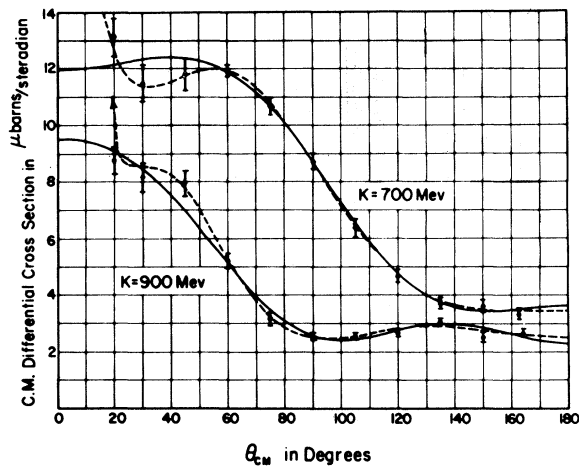


FIG. 2. Angular distributions of pions from $\gamma + p \rightarrow \pi^+ + n$ for 700- and 900-Mev photons.

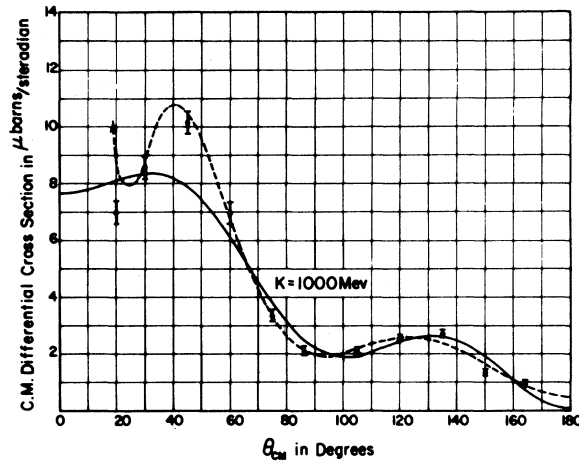


FIG. 3. Angular distributions of pions from $\gamma + p \rightarrow \pi^+ + n$ for 1000-Mev photons.

target spectrum based on an earlier pair-spectrometer measurement. Furthermore, for the 1000-Mev data at angles greater than 60°, the bremsstrahlung upper limit was lower than the maximum limit of acceptance for the spectrometer, and this necessitated corrections in resolution ranging from 3% at 75° to about 40% at the most backward angle. More detailed calculations will also be made of this effect.

Least-squares fits to the data are shown by the curves in Figs. 1-3. The solid curves are for expressions of the form

$$\frac{d\sigma}{d\Omega}(k, \theta) = A_0 + A_1 \cos\theta + A_2 \cos^2\theta + A_3 \cos^3\theta + A_4 \cos^4\theta.$$

Total cross sections obtained from the expression $\sigma_T = 4\pi(A_0 + A_2/3 + A_4/5)$ are shown in Table I, as are the coefficients A_0 to A_4 . The 1000-Mev data are not fitted well by the $\cos^4\theta$ expression, so that the total cross section shown in Table I is probably a little low. The dashed lines

represent least-squares fits of the form

$$(1 - \beta \cos\theta)^2 \frac{d\sigma}{d\Omega}(k, \theta) = B_0 + B_1 \cos\theta + B_2 \cos^2\theta + \dots + B_6 \cos^6\theta,$$

according to the prescription of Moravcsik.⁴

The extra freedom of the seven-coefficient expansion of Moravcsik gives a better fit than the five-coefficient expansion in $\cos\theta$, as might be expected. The 1000-Mev data seem to require a higher power than the $\cos^4\theta$ expression contains in order to obtain a reasonable fit.

The peak in the π^+ photoproduction cross section at 700 Mev has been reported before by both Cornell⁵ and CalTech¹ and has been interpreted as a resonance in a state of isotopic spin 1/2. Our cross sections are in agreement with those reported from Cornell⁵ at most of the points where they may be compared. The most interesting new feature of the present data is the remarkable change in the angular distribution between

Table I. Total cross sections and coefficients for $(d\sigma/d\Omega)(k, \theta) = \sum_{n=0}^4 A_n \cos^n\theta$.

Photon energy (Mev)	Total cross section ^a (microbarns)	Coefficients for fit in $\cos\theta$ (microbarns steradian)				
		A_0	A_1	A_2	A_3	A_4
600	89.9±1.2	+6.7±0.2	+7.7±0.5	+2.5±1.1	-4.1±0.7	-1.8±1.2
700	104.0±1.2	+8.7±0.2	+8.1±0.4	-1.6±1.1	-4.0±0.6	+0.7±1.1
800	66.0±0.9	+5.0±0.1	+3.2±0.3	-0.4±0.8	+0.3±0.5	+2.0±1.0
900	51.2±0.9	+2.6±0.1	+2.0±0.3	+6.3±0.7	+1.6±0.5	-2.9±0.8
1000	49.4±0.9	+2.2±0.1	+3.6±0.3	+10.5±0.6	+0.1±0.4	-8.8±0.7

^aSee text for explanation.

800 and 1000 Mev. The 1000-Mev distribution is so distinctive and this character appears so suddenly as the energy is increased, that we are tempted to ascribe it to a $T=1/2$, $J=5/2$ resonance first suggested in pion scattering data⁶ near an energy corresponding to photoproduction at 1100 Mev. This temptation is supported by two or three arguments. First, a $D_{5/2}$ state from magnetic quadrupole absorption or an $F_{5/2}$ state from electric quadrupole would have an angular distribution of the form $1 + 6\cos^2\theta - 5\cos^4\theta$ and this appears to be a major component in the 1000-Mev distribution, together with a strong $\cos\theta$ interference term. This interpretation is also useful for π^0 photoproduction, since the above angular distribution fits qualitatively the 940-Mev π^0 data of Vette² where the angular distribution was found to be different from that at all lower energies. A second, somewhat weak, point is that the total π^+ cross section shown in Table I does not continue to decrease appreciably between 900 and 1000 Mev, and this is consistent with a resonance at a somewhat higher energy, 1050 or 1100 Mev, which is just the energy expected from the pion scattering data.⁶

A possible difficulty is that the 1000-Mev data seem to require higher powers of $\cos\theta$ than the fourth, in order to achieve a reasonable fit. Perhaps the small-angle behavior can be explained by interference effects with the term in the photoproduction amplitude corresponding to interaction of the photon with the meson current. As Moravcsik has emphasized,⁴ this term should not be ignored, and an analysis including it is being attempted. No contribution of this term alone as distinct from interference effects is obvious in the data.

A complete report of this experiment, including the final corrections to the data discussed above, will be published later. We wish to thank Mr. Gerry Neugebauer for helping to take some of the final data.

*This work was supported in part by the U. S. Atomic Energy Commission.

¹F. P. Dixon and R. L. Walker, Phys. Rev. Lett. **1**, 142 (1958).

²J. I. Vette, Phys. Rev. **111**, 622 (1958).

³R. Gomez (private communication).

⁴M. J. Moravcsik, Phys. Rev. **104**, 1451 (1956).

⁵Heinberg, McClelland, Turkot, Woodward, Wilson, and Zipoy, Phys. Rev. **110**, 1211 (1958).

⁶Cool, Piccioni, and Clark, Phys. Rev. **103**, 1082 (1956).

POLARIZATION OF RaE ELECTRONS

H. Wegener, H. Bienlein, and H. v. Issendorff
Physikalisches Institut der Universität Erlangen,
Erlangen, Germany
(Received October 31, 1958)

For β -decay with $\Delta J=1$, yes, the longitudinal polarization P is $-v/c$, if the ξ -approximation is valid. The ξ -approximation gives an allowed spectrum. There is only one exception, RaE. Therefore one expects $P(\text{RaE}) \neq -v/c$. Theoretical investigations by Curtis and Lewis¹ and by Kotani and Ross² point out that $P(\text{RaE})$ should give information about time reversal at small energies and about matrix elements at larger energies. First measurements from Geiger *et al.*³ with Møller scattering and from Heintze *et al.*⁴ with Mott scattering after deflection by multiple scattering indicate that $|P(\text{RaE})| < v/c$, indeed. Unfortunately the energy discrimination in both measurements is too poor for a detailed conclusion.

We have measured $P(\text{RaE})$ for $E_{\text{kin}} = 120, 155, 209, \text{ and } 290$ keV by Mott scattering after deflection through an electric field. Figure 1 shows our experimental arrangements.⁵ The source Q is imaged to the receiving diaphragm of the spherical electric field by a thin magnetic lens. The end of the field (120° deflection) can be imaged to the scattering foil to avoid frame scattering. The depolarization by this lens has been measured earlier. Electrons which are once scattered in the scattering foil and then back-scattered by the walls are suppressed by

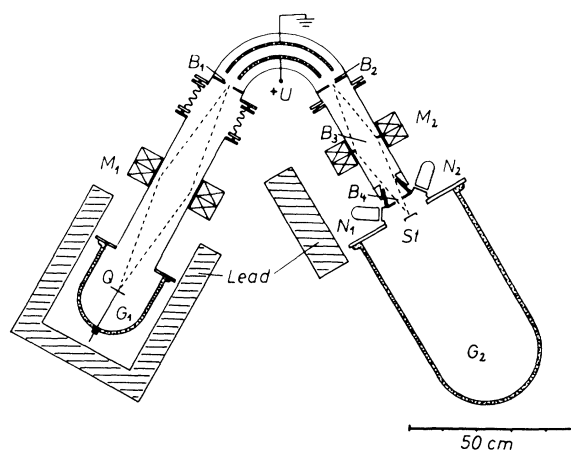


FIG. 1. Experimental arrangement. Q = source, M_1, M_2 = thin magnetic lenses, $B_1 - B_4$ = diaphragms, N_1, N_2 = counters, St - scattering foil, G_1, G_2 = glass cylinders; the other parts are of metal. The scattering part can be rotated. Lead = lead shielding.